Journal of Molecular Liquids 352 (2022) 118727

Contents lists available at ScienceDirect

Journal of Molecular Liquids

journal homepage: www.elsevier.com/locate/molliq

Theoretical and experimental insights about the adsorption of uranyl ion on a new designed Vermiculite-Polymer composite

Selçuk Şimşek [a,*], Savaş Kaya [a], Zeynep Mine Şenol [b], Halil İbrahim Ulusoy [c], K.P. Katin [d], Ali Özer [e], Nail Altunay [a], Ameni Brahmia [f,g]

[a] Sivas Cumhuriyet University, Faculty of Science, Department of Chemistry, 58140 Sivas, TÜRKİYE
[b] Sivas Cumhuriyet University, Zara Vocational School, Department of Food Technology, 58140 Sivas, TÜRKİYE
[c] Sivas Cumhuriyet University, Faculty of Pharmacy, Department of Analytical Chemistry, 58140 Sivas, TÜRKİYE
[d] Institute of Nanoengineering in Electronics, Spintronics and Photonics, National Research Nuclear University "MEPhI", Kashirskoe Shosse 31, Moscow 115409, RUSSIA
[e] Sivas Cumhuriyet University, Eng. Fac., Metallurgical and Materials Eng. Dept., 58140, Sivas, TÜRKİYE
[f] Chemistry Department, College of Science, King Khalid University, Abha 61413, Saudi Arabia
[g] Laboratoire des Matériaux et de l'Environnement pour le Development Durable, LR18ES10, University of Tunis El Manar, 2092, Tunisia

ARTICLE INFO

Article history:
Received 3 January 2022
Revised 28 January 2022
Accepted 7 February 2022
Available online 10 February 2022

Keywords:
Uranyl
Adsorption
Vermiculite
Composite
Density Functional Theory
Chemical Reactivity

ABSTRACT

A new Polyacrylamide (PAA)-Vermiculite (V) composite was synthesized and characterized with the help of FTIR, SEM, and PZC analyses. The effects of ion concentration, pH and ionic strength parameters to adsorption process were investigated in detail. The obtained data were analyzed and discussed in the light of the Langmuir, Freundlich and Dubinin-Radushkevich (DR) models. It was shown that the adsorption of UO_2^{2+} increased with the increasing of the pH while the increasing or decreasing of the ionic strength did not lead to significant changes in adsorption process. The adsorption of uranyl ion on new designed material followed an endothermic and spontaneous process with increased disorderliness at adsorbate/adsorbent interface. It was noticed that the adsorption process exhibits a pseudo-second-order kinetics. The interaction mechanism regarding to the interaction between uranyl ion and new designed Polyacrylamide (PAA)-Vermiculite (V) composite was highlighted in the light of Density Functional Theory (DFT) calculations. Both theoretical and experimental analyses made proved that the designed new material with a adsorption capacity of 0.375 mol kg^{-1} is a potential adsorbent for effective removal of uranyl ions from solutions.

1. Introduction

Removal of uranium species from environment and seawater is among of the important tasks of chemists in terms of both health and uranium recovery. Especially in the last century, with the spread of nuclear energy, which is hoped as clean energy, the increasing need for uranium has brought with it an increase in nuclear waste. In addition, the waste generated by laboratories and natural resources poses a threat to the environment and human health. Considering the average measured uranium concentration in seawater as 3.3 ppb [1], it can be said that its existence in some mediums is a serious threat to human health. It has been shown that if the daily dose is above 0.05 μg kg-1 body mass, it can be imagined that taken uranium ions will cause many health problems such as carcinogenic effects, renal failure, neurasthenia, infertility, leukaemia, and amentia [2].

Many methods are used for the removal/recovery of uranium species from waste and environmental waters. Filtration [3], biological treatment [4], precipitation [5] and adsorption are among the widely used methods for this aim. Adsorption technique is a physicochemical technique that stands out not only for uranium but also for removing many pollutants with its economical, practical, suitable adsorbent selection and speed features. One of the most preferred aspects of adsorption-based approaches is simplicity of procedure and reusability of adsorbent materials. For that reason, adsorption based approaches are useful and low cost in the removal of hazardous chemicals.

Clays [6], activated carbon [7], synthetic [8] and natural polymers [9] and composites [10] are commonly used materials as adsorbents in adsorption studies. In recent years, composite materials that are designed by combining good properties of a few materials became quite popular in this field. Composite materials

* Corresponding author.
E-mail address: simsek@cumhuriyet.edu.tr (S. Şimşek).

https://doi.org/10.1016/j.molliq.2022.118727
0167-7322/

that can be easily synthesized with the help of suitable experimental procedures exhibit high performance in terms of the selectivity, rapid adsorption and selectivity to target species. Use of natural materials like clay in synthesis of composite materials is also suitable with green chemistry principals because of the avoiding from much chemical substances. Although clays are among widely materials of adsorption studies, their using of clays is quite difficult because of the alkaline properties of their surface, coagulation/dispersion. On the other hand, composite materials obtained in a polymer matrix eliminate these negative features.

Vermiculite, a clay mineral, is a phyllosilicate with a 2:1 layered structure. The chemical formula of vermiculite is reported as (Mg, Fe^{2+}, Fe^{3+})3[(Al, Si)$_4O_{10}$](OH)$_2$·4H_2O. It is a low-cost, non-toxic, water-insoluble mineral, and abundant in nature [11]. Vermiculite is widely used to remove heavy metal contaminants from aqueous solutions, thanks to its high cation exchange capacity and small particle size and surface area.

In recent years, some important studies showing the effectiveness of the composite structures including vermiculite component were published. Gao and co-workers [12] prepared a new functionalized organo-vermiculite by combining the imidazole-ether-containing gemini surfactant into vermiculite. In the study, adsorption and co-adsorption of chlorophenols and Cr(VI) ion on the designed material were investigated. A recent paper penned by Weina and co-workers [13] showed that a multifunctional polyethylene-imine-graphene oxide/organo-vermiculite composite is quite effective in the removing of azo dyes.

In the present paper, a useful, low-cost, water-insoluble polymer/mineral adsorbent system was designed as a combination of polyacrylamide (PAA) polymer and vermiculite (V) mineral. The novelty of the present study is that this new combined material exhibits high performance for the effective removal of uranyl ion the aqueous medium. The adsorption capacity of the new material can compete with the popular adsorbents in the literature.

2. Materials and methods

2.1. Chemicals

In this study, Vermiculite (V) was purchased from Akmin Mining (Ankara). $(CH_3COO)_2UO_2·2H_2O$, and 4-(2-pyridylazo) resorcinol (PAR) were purchased from Merck (Germany). Other chemicals used in this study: Acrylamide monomer (AA), Ammonium persulphate (APS), N, N′ - methylenebisacrylamide, N, N, N′, N′ tetramethylenediamine (TEMED), HCl, NaOH, KNO_3 and C_2H_5OH. In all experiments made, distilled water was used.

2.2. Preparation of UO_2^{2+} solutions and concentration determination

5000 mgL^{-1} UO_2^{2+} stock solution was prepared with dissolution of $(CH_3COO)_2UO_2·2H_2O$ Working solutions were prepared by dilution of the stock UO_2^{2+} solution with distilled water. The UO_2^{2+} concentrations were analyzed by UV–vis spectrophotometer (SHIMADZU, 160 A model, Japan). The concentration of UO_2^{2+} was determined by the absorbance measurement and by using the PAR method [14]. In PAR method, concentrations of UO22 + ions are determined obtaining spectrophotometrically a selective complex with PAR at λ = 530 nm.

2.3. Preparation of PAA-V composite material

PAA-V composite was synthesized via aqueous solution polymerization method. 2 g AA monomer was dissolved in 10 mL of distilled water. 1 g of V in 10 mL of distilled water was dispersed in the monomer solution mentioned above. 0.2 g in 10 mL of distilled of cross linker N, N′ methylene bisacrylamide was dissolved in the AA-V mixture solution. Then, TEMED (400 μL) and initiator APS (1 g) were added as described in the literature [15]. After completion of the polymerization, the obtained new composite was washed with distilled water to remove any impurities, subsequently, dried at 40 °C, ground (50 mesh), thus a powdered PAA-V composite material was obtained

2.4. Characterization of the PAA-V composite material

2.4.1. FT-IR analysis

FT-IR analysis enables to determine the specific functional groups of PAA-V and its components. FT-IR analysis was recorded using the FT-IR spectrophotometer (Perkin Elmer 400), the analysis was done over a wavelength range of 400–4000 cm^{-1} with KBr pellets.

2.5. SEM-EDX analysis

The surface morphology and chemical composition of PAA-V and its components were characterized by using SEM-EDX analysis with Mira3 XMU Tescan (Czechia) and x-act Onca Oxford Inat.(UK).

2.6. The point of zero charge (PZC)

To determine the PZC values of PAA-V composite, the pH of 0.1 mol L^{-1} KNO_3 solution was adjusted in the range between 1.0 and 12.0 with the help of HCl or NaOH (0.1 mol L^{-1}) solutions, then, 100 mg of PAA-V was added and the final pH values were measured after 24 h. The initial pH values were plotted against ΔpH to obtain PZC.

2.7. Adsorption procedure

Adsorption experiments were done by using batch method. The effects of the parameters such as solution pH, initial UO_2^{2+} concentration, contact time, temperature and desorption on adsorption process were investigated with the help of required experimental processes. All experiments were carried out at constant concentration of 1000 mg L^{-1} UO_2^{2+} in 10 mL solutions in 10 mL polypropylene tubes containing 100 mg PAA-V at a shaking rate of 150 rpm. The details of experimental conditions are given in Table 1. The concentration of UO_2^{2+} was determined by the absorbance measurement. Adsorption% and Q (mol kg^{-1}) values were calculated from the following formulae.

$$Adsorption\% = \left[\frac{C_i - C_f}{C_i}\right].100 \quad (1)$$

$$Q = \left[\frac{(C_i - C_f)V}{m}\right] \quad (2)$$

In these equations; C_i is the initial concentration (mg L^{-1}), m stands for the adsorbent mass (g), C_f is equilibrium concentration (mg L^{-1}), and V is the solution volume (L).

2.8. Desorption procedure

Batch systems were used in the desorption processes in order to evaluate the re-use efficiency. The re-use efficiency is consisted of accelerated three adsorption/desorption runs. The PAA-V (100 mg) was added to polypropylene tubes containing 10 mL HCl, NaOH, HNO3 and ethyl alcohol (each one, 0.1 mol L^{-1}) solutions and at a shaking rate of 150 rpm for 24 h. The solutions were centrifuged at 5,000 rpm for 10 min and the supernatant concentration was

Table 1
Batch experimental conditions for adsorption of UO_2^{2+} onto PAA-V.

Aim of experiment	Solution pH	Initial UO_2^{2+} conc. (mg L^{-1})	Contact time (min)	Temperature (^{0}C)
Effect of pH	1.0–7.0	1000	1440	25
Effect of concentration	4.5	50–1000	1440	25
Effect of time	4.5	1000	2–1440	25
Effect of temperature	4.5	1000	1440	5, 25, 40
Desorption	4.5	1000	1440	25

subsequently measured by UV–vis spectrophotometric method. % Desorption was calculated using the Equation (3).

$$Desorption\% = \frac{Q_{des}}{Q_{ads}}.100 \quad (3)$$

wherein, Q_{des} and Q_{ads} represent the desorbed and adsorbed amount of UO_2^{2+} in mol kg^{-1} unit, respectively.

2.9. The assessment of adsorption isotherms

For the analysis of adsorption process, Langmuir [16], Freundlich [17] and Dubinin -Radushkevich (D-R) [18] isotherm models were used. In the light of these models, the adsorption mechanism, the binding energy for the interaction between the adsorbate and the adsorbent and adsorption capacity were determined. The equations regarding to Langmuir, Freundlich and Dubinin –Radushkevich isotherms are given as, respectively.

$$Q = \frac{X_L K_L C_e}{1 + K_L C_e} \quad (4)$$

$$Q = K_F C_e^{\beta} \quad (5)$$

$$Q = X_{DR} e^{-K_{DR}\varepsilon^2} \quad (6)$$

In these equations; Q (mol kg^{-1}) is the amount of adsorbed UO_2^{2+}, K_L is a parameter regarding to adsorption energy in Langmuir isotherm and C_e is the equilibrium concentration (mol L^{-1}). K_F: Freundlich constant, β: adsorbent surface heterogeneity and X_L is the maximum adsorption capacity, X_{DR} is a measure of adsorption capacity, K_{DR} is the activity coefficient (mol^2KJ^2) and ε is the Polanyi potential, R is the ideal gas constant (8.314 J $mol^{-1}K^{-1}$) and T is the absolute temperature (K). The Polanyi potential (ε) is calculated from the following formula.

$$\varepsilon = RT\ln\left(1 + \frac{1}{C_e}\right) \quad (7)$$

In Dubinin Radushkevich model, the adsorption energy (E_{DR}) is calculated as:

$$E_{DR} = (2K_{DR})^{-0.5} \quad (8)$$

It is important to note that E_{DR} is used whether the interaction is physical or chemical. If the adsorption energy calculated is between 8 and 16 kJ mol^{-1}, the adsorption is chemical. If the adsorption energy is smaller than 8 kJ mol^{-1}, the adsorption is physical.

2.10. The calculation of adsorption kinetics

Three commonly used kinetics models were considered to determine the adsorption kinetics such as the pseudo first order (PFO) [19], pseudo second order (PSO) [20], and intra particle diffusion (IPD) [21]. The equations regarding to the mentioned models are given below.

$$Q_t = Q_e[1 - e^{-k_1 t}] \quad (9)$$

$$Q_t = \frac{t}{\left[\frac{1}{k_2 Q_e^2}\right] + \left[\frac{t}{Q_e}\right]} \quad (10)$$

$$Q_t = k_i t^{0.5} \quad (11)$$

In the given equations, Q_t (mol kg^{-1}) is the adsorbed amount at time t (min). Q_e (mol kg^{-1}) is the adsorbed amount at equilibrium. k_1, k_2 and k_i are the rate constants of the PFO (min^{-1}) model, the PSO model (mol^{-1} kg min^{-1}) and the IPD (mol^{-1} kg $min^{-0.5}$) model, respectively.

In the PFO and PSO models, the initial adsorption rates are calculated from the following equations, respectively.

$$H_1 = k_1 Q_e \quad (12)$$

$$H_2 = k_2 Q_e^2 \quad (13)$$

where, H_1 and H_2 represent the initial adsorption rates via PFO and PSO models, respectively.

2.11. The calculation of adsorption thermodynamics

Calculated thermodynamic parameters are quite useful to see whether adsorption process is spontaneous. In addition to this, we can easily show the temperature effect on the the UO_2^{2+} adsorption onto PAA-V composite thanks to thermodynamic parameters. For the calculation of ΔH^0 (enthalpy), ΔS^0 (entropy) and ΔG^0 (Gibbs free energy) parameters regarding to the adsorption process, we used the following equations.

$$K_D = \frac{Q}{C_e} \quad (14)$$

$$\Delta G = -RT\ln K_D \quad (15)$$

$$\ln K_D = \frac{\Delta S^0}{R} - \frac{\Delta H^0}{RT} \quad (16)$$

$$\Delta G^0 = \Delta H^0 - T\Delta S^0 \quad (17)$$

3. Results and discussion

3.1. Characterization of the studied material

The FTIR spectra of regarding to V, PAA and PAA-V systems are given in Fig. 1. The broadband at 1000 cm^{-1} in the spectrum belongs to Vermiculite and is due to asymmetric Si—O—Si and Si—O—Al stretching vibrations. The peak in 1644 cm^{-1} is assigned to the deformation of OH groups in water. In addition, the peak at 3388 cm^{-1} is assigned to the interlayer water in vermiculite. These peaks are characteristic peaks of the Vermiculite structure. The peaks at 2950, 1600–1700 and 1000–1200 cm^{-1} belong to CH, COOH and CN groups, respectively. The peak at 2943 cm^{-1} in new synthesized PAA-V material is the proof the existence of PAA organic component. Furthermore, the deformation at 1421

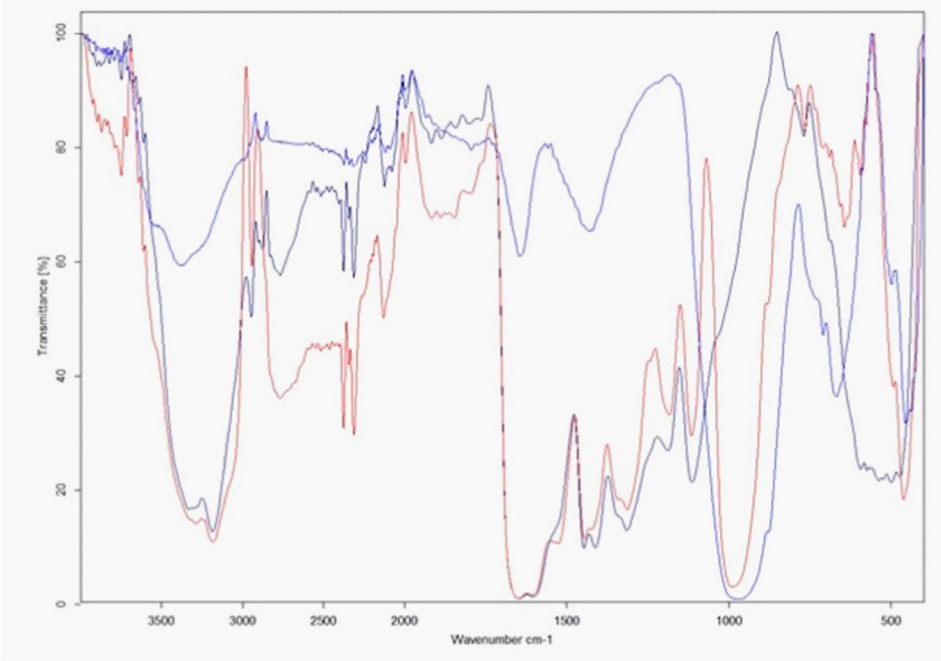

Fig. 1. FTIR spectra of V, PAA and PAA-V (Black: PAA, Blue: V, Red: PAA-V).

and 1444 cm^{-1} peaks support the existing of vermiculite in the new designed composite.

3.2. SEM and EDX spectra

As seen from Fig. 2, Vermiculite particles were about 5–100 μm fine and the mineral contains hard and fragile particles as well as layered silicate particles of irregular round shape. The fractured porous particles can be seen as well as layered particles on the upper right of higher magnification image of Vermiculite (5kX). The cleavage planes of vermiculite sharp particles, which may be of Afwillite and Margarite 2 M1 phase. Polyacrylamide crushed particles were seen in PAA abbreviated image. PAA has amorphous glassy smooth surface with crushed and cleavage cracks that

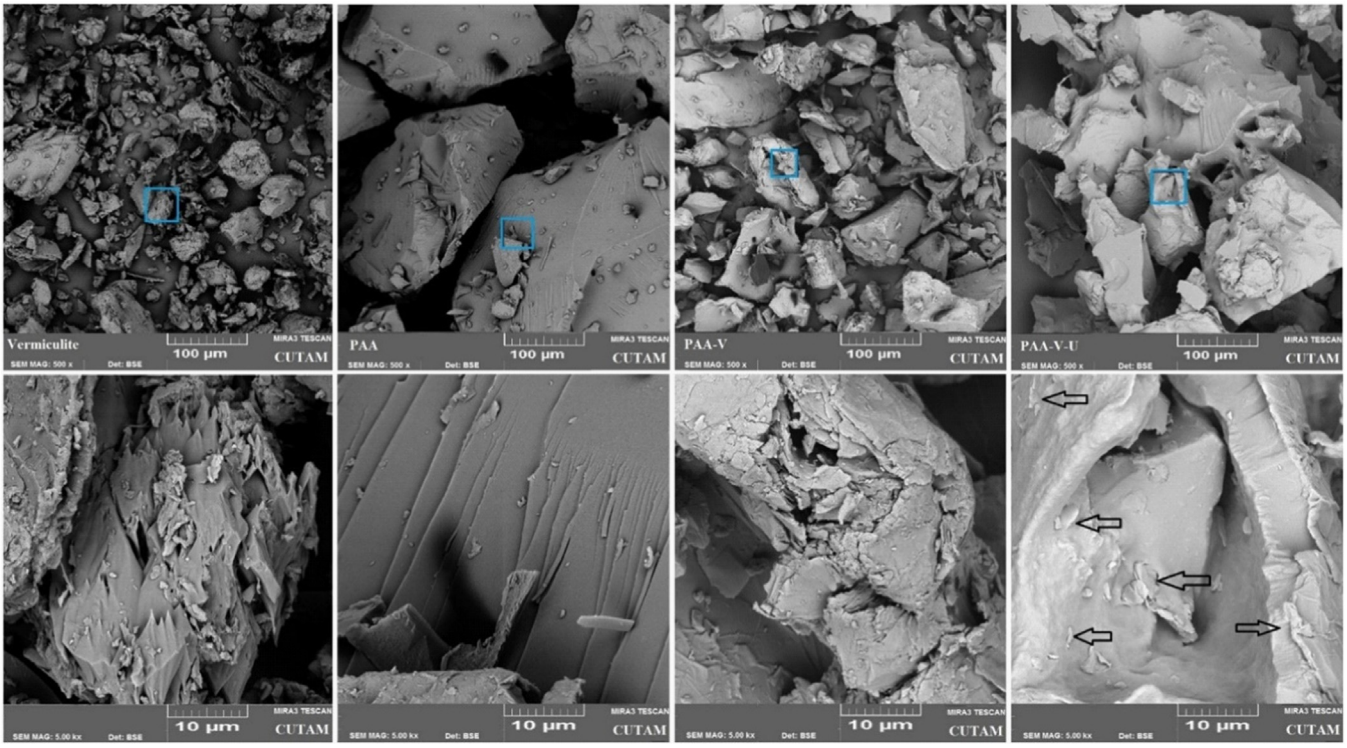

Fig. 2. SEM-BSE images of vermiculite, polyacrylamide, PAA-V composite and U adsorbed PAA-V composite on the upper row, the lower low indicates the higher magnification images (blue squares) of as mentioned material right above them.

indicate the semi-crystalline structure. The PAA particles were also seen as a few 100 μm particles that can only be dissolved in its solvent and produces a long chain polymer solute. After dissolution in water and precipitation with vermiculite phase, average particles size of PAA-V composite as compared with pure vermiculite increased. This phenomenon is known as steric entrapment of cationic surfaces with nonpolar polymer structures.

Fig. 3 (a) indicates the SEM-BSE images of pure V, PAA-V and PAA-V-U composites with corresponding EDX elemental analysis, respectively. Vermiculite is a mixture of Mg-K-Ca-Al-Fe-Si-OH groups which was also shown in XRD phase analysis. Trace amounts of Ti is also seen in EDX results. A combined mixture of Grossite 2 M and Afwalite as well as alumina silicate layered groups. Average powder size was estimated to 23 ± 6 μm with observable layers in the powders from SEM.

Fig. 3 (b) shows the SEM image of PAA-V composites with EDX elemental analysis. The smoothened surface and closed layers may be attributed to PAA sorption onto and into vermiculite layers. A

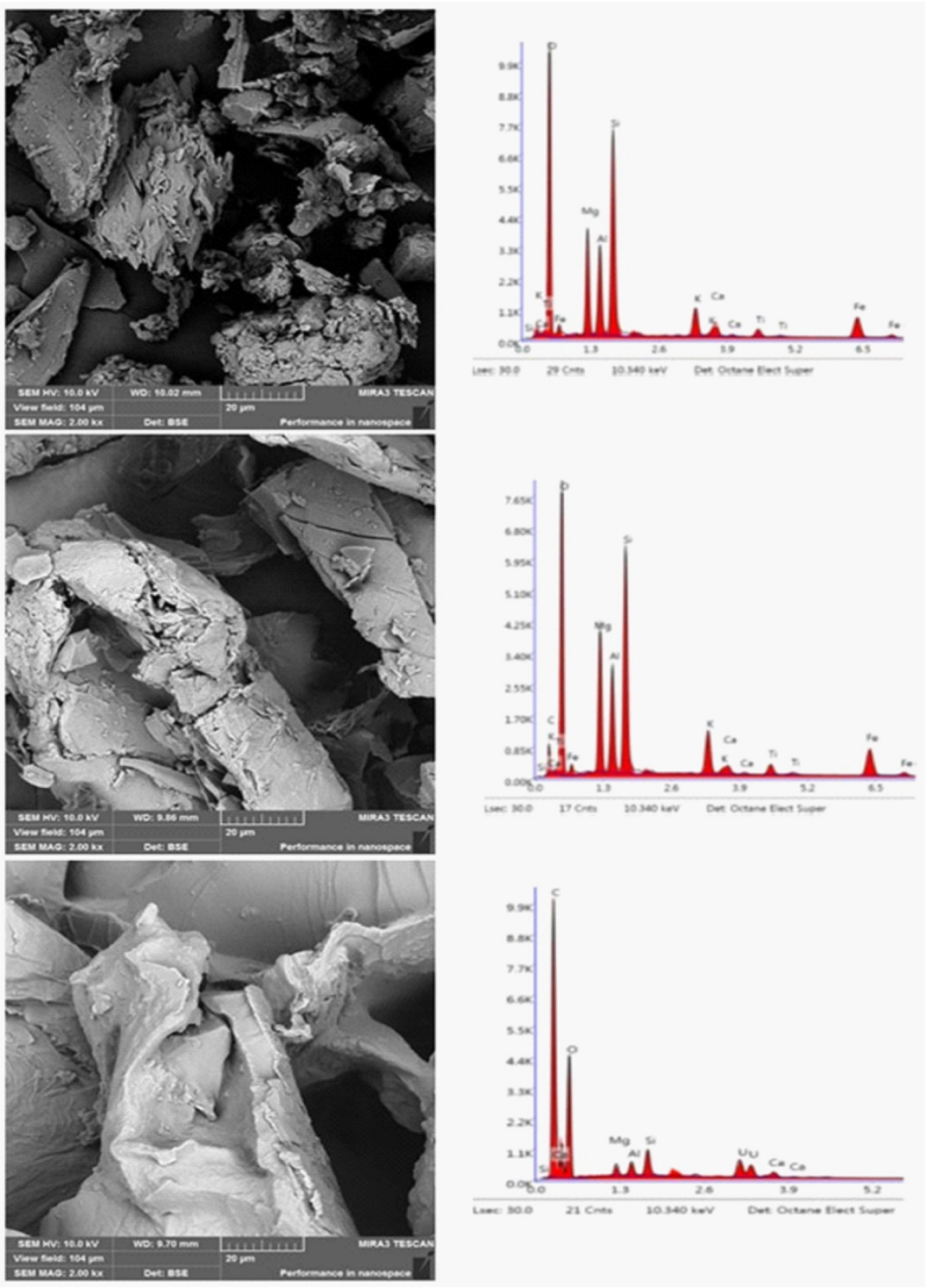

Fig. 3. EDX view of structures.

certain amount of agglomeration in V particles is seen due to PAA doping on the surfaces, and this favors the agglomeration. The sudden increase in particle size up to 78 ± 24 μm is inevitable. Due to PAA surface sorption, carbon elemental analysis is seen as increased in EDX analysis with other elements of interest. Especially, the peak intensity of Si and O elements decreased according to pure form, which may be attributed to the silicate interlayer doping of PAA, while the other elements remained partially constant.

Fig. 3(c) presents the U doped PAA-V composites. As can be clearly seen, the very smooth surface with agglomerated particles is evident due to PAA coating as well as uranyl acetate coating. Since uranyl adsorption is specified high, the corresponding EDX elemental analysis affected the peak intensities of Si-O-Mg-K-Fe-Ca while Ti peak was disappeared totally. When the elements' peaks were decreased, C peak was increased to the highest intensity due to PAA and acetate roots due to thickness of U coating. Coating of U occurred as intercalation between layers and these layers were stacked together.

3.3. PZC value and the influence of pH to adsorption

It is well-known that, one of the most important parameters in the adsorption of ions from the aqueous solution is the pH of the solution. The change in the H^+ concentration in the solution affects both the ion type in the solution and the charge character of the adsorbent surface. Many valuable studies reported in the literature showed how pH effects the adsorption process [22,23]. It can be seen from these studies, at some pHs, adsorption decreases or does not occur while adsorption takes place at certain pHs. There are two reasons for this phenomenon. The first is that the type of the relevant ion in the solution, and hence the charge, changes with the changing pH of the solution. The formation of different ions in different pHs effects directly the adsorption process. Second reason is that changing solution pH can change the surface charge of the interface where adsorption will take place. As a result, adsorption amount may change with the changing of repulsion and pull forces that will occur between the adsorbate/adsorbent. Therefore, it is very important to determine the pH at which an adsorbent is used effectively or the highest efficiency of adsorption is obtained in order to ensure the best adsorption.

One of the most practical methods used to determine the adsorbent surface charge is to find the charge of the surface at different pHs by interacting the adsorbent with solutions at different pHs without adsorbate at constant ionic strength, using the initial and equilibrium pH. The paper published by Cerovic and coworkers [24] reported that in dense proton and hydroxyl solutions, the adsorbent surface tries to establish a balance between ion exchange and solid solution. Considering this pH change, the zero charge point of the surface can be easily found. The PZC value is accepted as the value at which the total net charge on the surface is zero [25]. To determine the surface charge and zero point of the PAA-V composite, a series of experiments were carried out and the results are visualized in Fig. 4. The empirically determined PZC value for the composite is 6.41, at which the total net charge is equal to zero. Below this point, the surface charge is predominantly positive, but this does not mean that the surface is completely positive in this region. At pH above PZC, the surface charge is predominantly negative, and the negative charge increases with increasing pH.

In order to investigate the effect of solution pH on the adsorption of uranyl ions, a series of experiments were carried out with solutions containing fixed uranyl ions with different initial pHs. Obtained results are visually given in Fig. 5. Initial pH adjustments were made using HCl acid and NaOH. The pH range chosen in the study is 1–7 because various types of poly-anionic hydroxides such as $UO_2(OH)_4^{2-}$, $UO_2(OH)_5^{3-}$ and $UO_2(OH)_4^{2-}$], which are formed by uranium in the alkaline region, cause precipitation [26]. As can be seen from the Fig. 2, a clear increase in adsorption was observed with increasing pH. This result is related to both the type of the ion in this pH range and the variation of the surface charge found in the PZC study. Although the dominant type of uranyl ions in this region is the hexavalent uranium cation, the formation of polycationic species such as UO_2OH^+, $(UO_2)_2(OH)_2^+$, $(UO_2)_3(OH)_5^+$ changes the adsorption as the pH increases [27]. The surface charge changes from cationic to anionic with increasing pH. It is concluded that the increase in the presence of negative groups on the surface increases the adsorption of uranyl ions, in which cationic species are dominant.

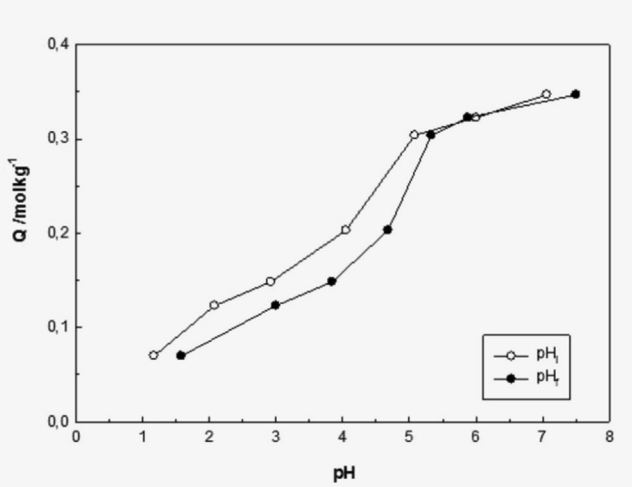

Fig. 4. Effect of pH on the adsorption of UO_2^{2+} onto PAA-V.

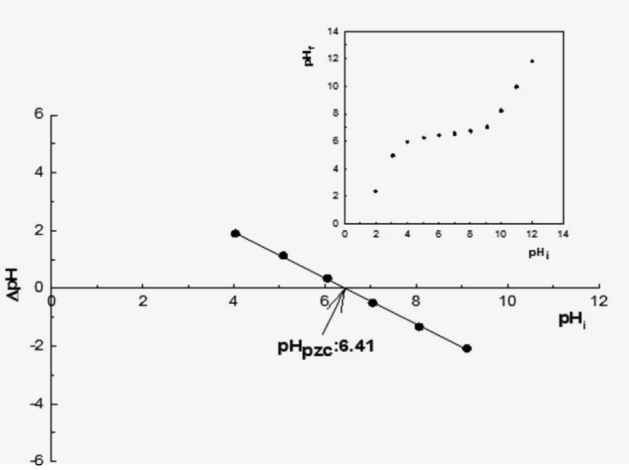

Fig. 5. PZC plots of the PAA-V in range of pH 2.0–12.0.

4. Effect of uranyl concentration to adsorption

Because the adsorption process is a very complex, the optimization of adsorption parameters such as adsorption capacity, adsorption energy, adsorbent surface heterogeneity is quite important in terms of the accurately analysis of the adsorption. The commonly used method to find the adsorption capacity is to use the isotherms drawn with the adsorbed amount against the equilibrium concentration, after the equilibrium is reached by the interaction of the adsorbate and a fixed amount of adsorbent at different initial

concentrations. Among the isotherms with very different characteristics, the most common type of isotherm is the isotherm, which gives a hyperbola curve that reaches a plateau after the amount of adsorbed increases up to a certain equilibrium concentration. After reaching to the equilibrium at these isotherms, the maximum adsorption capacity can be found by extrapolation from the plateau. In fact, various mathematical curve equations used in the analysis of this curve correspond to widely used adsorption models such as Langmuir, Freundlich, DR. Each of these models tries to find adsorption parameters with different assumptions about the adsorbent or adsorption process. For example, the Langmuir model assumes that the surface is homogeneous and consists of a certain number of active sites, and predicts that the monolayer adsorption capacity, in other words, the maximum adsorption capacity can be found from the plateau. The Freundlich model describes the surface with a heterogeneity factor and tries to explain it with an exponentially decreasing energy domain distribution. The DR model accepts that adsorption energy can be considered as a measure in determining whether adsorption is chemical or physical rather than the amount of adsorption. A series of experiments were carried out for the adsorption parameters of the PAA-V composite, which was shown to be formed by the newly synthesized vermiculite with polymer and can be used as an adsorbent for uranyl ions. The analytical results were given in Fig. 6. The compatibility of various adsorption models to this isotherm has been investigated. Table 2 includes the model parameters of Langmuir, Freundlich and Dubinin-Radushkevich isotherms.

Composite uranyl ion conforms to the L-type adsorption isotherm in the Giles classification of adsorption. The maximum adsorption capacity can be found from the fit of the isotherm to the Langmuir model. Comparing our results with the literature values, it can be said that our material is an average adsorbent. Designing a composite material, we obtained an adsorbent with large surface area and practical to use. Due to the inert property of the polymer, the adsorption property of the adsorbent is entirely due to the active surfaces of vermiculite and the increase in these active surfaces.

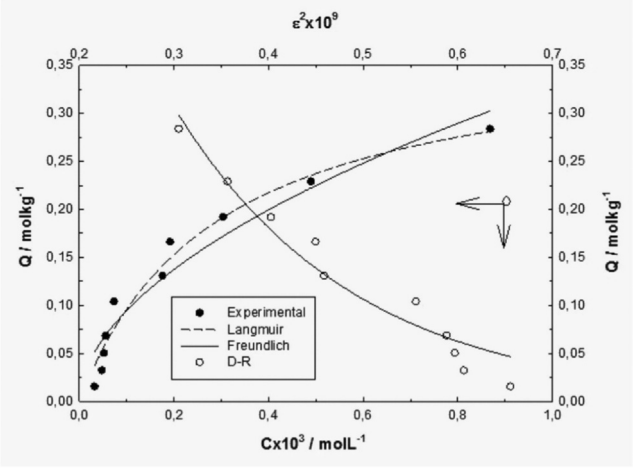

Fig. 6. The experimentally obtained adsorption isotherms of UO_2^{2+} onto PAA-V.

4.1. The kinetic parameters of adsorption

One of the factors affecting the completion of the adsorption process is the interaction time of the solid phase with the solution. Defining the adsorption kinetic model is quite important for both for estimating the adsorption completion time and for predicting the concentration of the species that moves to the solid phase and remains in solution after a certain time. The appropriate model makes it possible to determine both the kinetic rate constant and the estimation of the adsorbed amount at equilibrium.

Among the events taking place at the interface, there are many steps such as transfer of ions or molecules to the surface, film formation on the surface, diffusion to the pores, and binding to active groups. The difference in the realization time of these steps affects the time for the adsorption to reach equilibrium. Therefore, each step should be defined with the appropriate kinetic model. In recent years, Lagergren (pseudo first order), pseudo second order, intra particle diffusion and Elovich models have been widely used kinetic models in the field of adsorption. Especially PFO, PSO, IP models are widely used to describe the adsorption process in porous structures.

In order to determine the suitable kinetic model for this study and to find the kinetic parameters, adsorption measurements were made at constant ion concentration and at different times. Obtained results are visually given in Fig. 7. The compatibility of different kinetic models with these experimental results was investigated. The kinetic parameters obtained are given in Table 3. The obtained results show that the adsorption process fits both the PFO and the PSO model. Although R^2 values implies that the PSO model is more suitable, the predictability of the amount adsorbed at equilibrium was found to be approximately the same for both models. However, considering the theoretical acceptances on which both the PFO and the PSO model are based, it can be concluded that the PSO model is more appropriate. It is important to note that the predictability of kinetic parameters in solutions with

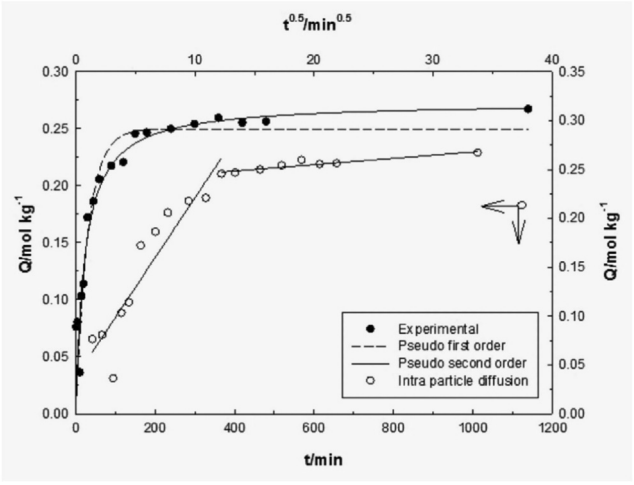

Fig. 7. Compatibility of experimental adsorption data with the considered kinetic models.

Table 2
Langmuir, Freundlich and Dubinin-Radushkevich isotherm models parameters.

Langmuir			Freundlich			Dubinin-Radushkevich			
X_L	K_L	R^2	K_F	n	R^2	X_{DR}	$-K_{DR}x10^9$	E_{DR}	R^2
0.375	3441	0.968	13.3	0.537	0.868	1.50	5.29	9.73	0.948

X_L (molkg^{-1}), K_L (Lmol^{-1}), X_{DR} (molkg^{-1}), $-K_{DR}x10^9$ (mol^{2}KJ^{-2}), E_{DR} (kJ mol^{-1})

Table 3
The kinetic parameters obtained via PFO and PSO models for UO_2^{2+} adsorption onto PAA-V.

UO_2^{2+}	$(k_1, k_2, k_i)x10^3$	R^2	Q_T	Q_E	$Hx10^3$
PFO	32	0.913	0.250	0.255	2.9
PSO	157	0.930	0.272	0.255	19
Weber-Morris					
Surface adsorption	29.8	0.953			
İntra particle diffusion	0.78	0.300			

k_1 (dk^{-1}), k_2 (mol^{-1} kg min^{-1}), and k_i (mol kg^{-1} min^{-1}) are the rate constants. Initial adsorption rate, H (mol kg^{-1}min) for pseudo-second-order is calculated from $H = k_2Q_e^2$

low initial concentrations is more successful with the PSO model while the ability of the PFO model to predict kinetic parameters is high in adsorptions with high initial concentrations.

4.2. Thermodynamics parameters

To investigate the thermodynamic behaviour of the adsorption, the results obtained by adsorption process at different temperatures in the fixed ion concentration and adsorbent mass are presented in the Fig. 8. Thermodynamic parameters like ΔH, ΔS and ΔG predicted using van't Hoff equation. of the adsorption process are given in Table 4.

Negative ΔH value indicates that the adsorption process is exothermic, that is, pre-adsorption interactions are stronger than post-adsorption interactions. The adsorption entropy increases as expected in the case of adsorption from the solution. This is an indication of the increase in disorder in all events occurring between solid–liquid. It also includes the secondary interactions that occur with adsorption throughout the adsorption. For example, events such as dehydration, ion exchange, post-adsorption interaction of water molecules lead to an increase in adsorption entropy, in contrast to adsorption from the gas phase. The free energy value is negative as expected, which means that the event occurs spontaneously.

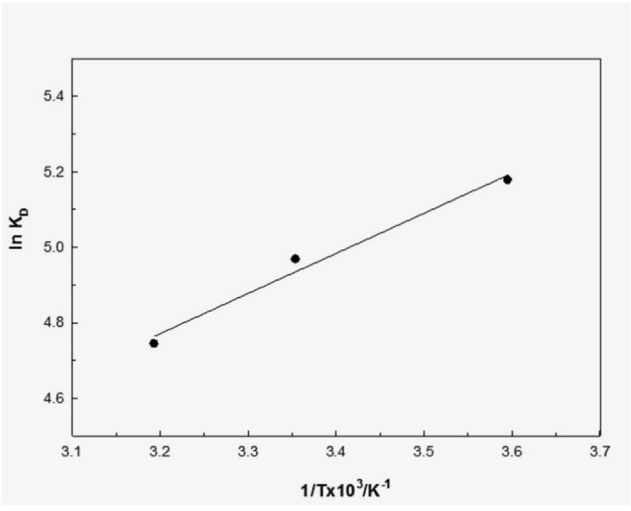

Fig. 8. Influence of temperature to adsorption process.

Table 4
The thermodynamic parameters for UO_2^{2+} adsorption.

ΔH/kJmol^{-1}	ΔS/Jmol^{-1}K^{-1}	ΔG/kJmol^{-1}	R^2
−8.85	11.34	−12.2	0.982

4.3. Effect of ionic strength

One of the factors affecting adsorption is the salt concentration of the solution. Many studies have shown that the salt concentration in the solution changes the amount of adsorption. Changing of the salt concentration may result with the increasing, decreasing or not affecting the adsorption depending on the interaction type of adsorbed uranyl ions with the surface. Hao and coworkers [28] explained the effect of ionic strength on adsorption in two ways. (I) A decrease in adsorption is observed as a result of the competition with the increasing salt concentration of the outer-sphere complexes formed by the adsorbed species in the adsorption centers on the surface. (II) Increasing of salt concentration affects the activity coefficient of the adsorbed ion, which is effective in the transfer of ions to the surface. It can be easily seen from Fig. 9 that the adsorption of uranium on the composite is not affected by the change in ionic strength. This situation showed that the adsorbed species is retained on the surface by a complex formation mechanism rather than an ion exchange mechanism, and since salt concentration does not affect the metal activity coefficient, it has no effect on the transfer to the surface [29].

4.4. Theoretical modeling of the interaction of UO_2^{2+} with new composite

Corrosion inhibition studies include the analysis of adsorption characteristics of inhibitor molecules against the corrosion of various metal surfaces. In addition to experimental approaches,

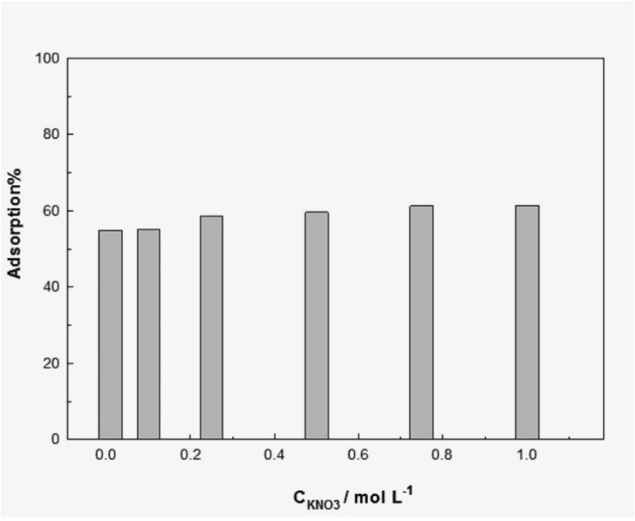

Fig. 9. Effect of ionic strength to adsorption.

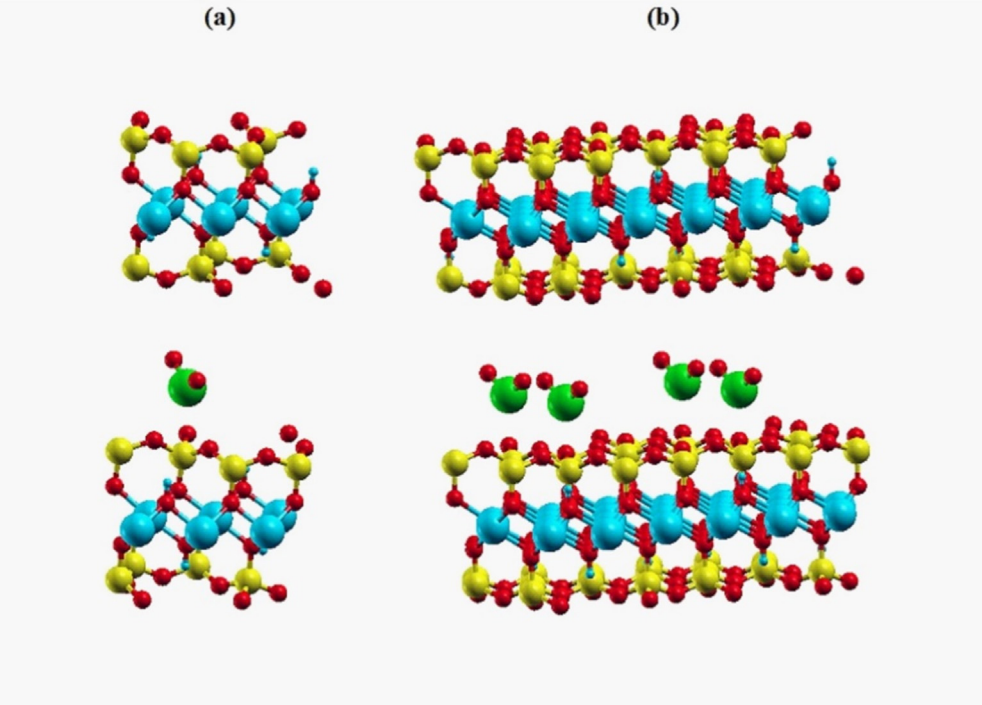

Fig. 10. Optimized geometry of UO_2-doped vermiculite: unit cell (*a*) and 2x2 cells (*b*). Red, yellow, blue and green balls depict oxygen, silicon, magnesium and uranium atoms, respectively. Small blue balls depict hydrogen atoms.

Density Functional Theory calculations are also considered to predict the corrosion inhibition performances of organic and inorganic molecular systems. Many corrosion inhibition studies including both theoretical and experimental analyses are available in the literature [30–33].

Vermiculite was represented as a $Mg_{12}Si_{16}O_{48}H_8$ unit cell considered under periodic boundary conditions. Optimized parameters of its monoclinic lattice are a = 5.31 Å, b = 9.20 Å, c = 28.46 Å, γ = 97.1°. For performed DFT [34,35] calculations, we applied GGA-PBE functional [36] combined with scalar-relativistic ultra-soft projector augmented wave pseudopotentials generated by Dal Corso, as it is implemented in Quantum Espresso software [37]. Selected calculation level is widely preferred in the highlighting of the nature of the interactions between chemical systems [38,39]. Cutoff energies for wave functions and for the charge density were chosen to be 100 and 800 Ry, respectively. Grimme's dispersion corrections D3 were taken into account [40]. A Monkhorst-Pack k-point grid of 8 × 8 × 8 was used.

UO_2^{2+} was initially placed between vermiculite layers and then geometry of UO_2^{2+}-doped system was optimized (Fig. 10). Binding energy E_b was calculated as $E_b = E(Mg_{12}Si_{16}O_{48}H_8) + E(UO_2^{2+}) - E(UO_2^{2+}\text{-}Mg_{12}Si_{16}O_{48}H_8)$. We found that optimal position for uranium atom is strongly above the Si atom. The distances between uranium and three the nearest oxygen atoms are equal to 2.85 Å, indicating non-covalent bonding. The value of E_b = 0.074 eV confirms that the interaction is van-der-Waals in its nature.

Chemical hardness [41,42] is reported as the resistance against electron cloud polarization of chemical systems. Hard and Soft Acid-Base Principle introduced by Pearson [43] in 1960 states that hard acids prefer to interact with hard bases and soft acids prefer to interact with soft bases. Oxidation number of uranium in uranyl ion is + 6. This system exhibits hard character according to HSAB Principle. It is seen from the structure of vermiculite that this system includes many hard atoms in its molecular structure. For that reason, polyacrylamide vermiculite acts an effective adsorbent for the adsorption of uranyl ion.

5. Conclusions

In recent years, composite materials including a few components are widely used in the removing of hazardous chemical structures. This paper includes the synthesis and introducing of a new PAA-V composite material. The new material has been characterized through SEM-EDX and FT-IR methods. The adsorption capacity of the new composite was investigated in the light of some important experimental and theoretical analyses. The obtained results proved that new PAA-V composite will be quite useful for the effective removal of uranyl ions. The adsorption capacity of the composite was noted as 0.375 mol kg^{-1}. It was noted that adsorption process is affected from the pH of the solution. It was reported that the in this study, PSO model of adsorption kinetics is suitable, the enthalpy of adsorption is negative, the entropy is positive, and adsorption occurs spontaneously at the operating temperature. Chemical hardness is one of the most popular parameters showing the power of the interactions between chemical species. The interaction between composite material and hexavalent uranium in solution is supported with Hard and Soft Acid-Base Principle. It is proved that polyacrylamide vermiculite is an effective adsorbent for hard ions like UO_2^{2+}.

CRediT authorship contribution statement

Selçuk Şimşek: Conceptualization, Methodology, Supervision. **Savaş Kaya:** Software, Writing – review & editing, Visualization. **Zeynep Mine Şenol:** Methodology. **Halil İbrahim Ulusoy:** Methodology. **K.P. Katin:** Software, Writing – review & editing, Visualization. **Ali Özer:** Methodology. **Nail Altunay:** Methodology. **Ameni Brahmia:** Funding acquisition, Writing – review & editing.

Declaration of Competing Interest

The authors declare that they have no known competing financial interests or personal relationships that could have appeared to influence the work reported in this paper.

Acknowledgements

The authors extend their appreciation to the Deanship of Scientific Research at King Khalid University for funding this work through research groups program under grant number R.G.P.2/71/42.

The present study (Project no: F-509) was also supported by Cumhuriyet University Scientific Research Projects Commission (CUBAP), Sivas in Turkey. The authors have declared no conflict of interest.

References

[1] Nordberg, G. F., Fowler, B. A., Nordberg, M., & Friberg, L. (2007). Handbook on the toxicology of metals. Academic press Amsterdam, p: 1024

[2] M. Bergmann, O. Sobral, J. Pratas, M.A.S. Graça, Uranium toxicity to aquatic invertebrates: a laboratory assay, Environ. Pollut. 239 (2018) 359–366.

[3] B. Yu, G. Ye, J. Chen, S. Ma, Membrane-supported 1D MOF hollow superstructure array prepared by polydopamine-regulated contra-diffusion synthesis for uranium entrapment, Environ. Pollut. 253 (2019) 39–48.

[4] U.K. Banala, N.P.I. Das, S.R. Toleti, Microbial interactions with uranium: Towards an effective bioremediation approach, Environ. Technol. Innovation 21 (2021) 101254, https://doi.org/10.1016/j.eti.2020.101254.

[5] P. Li, B. Zhun, X. Wang, P. Liao, G. Wang, L. Wang, Y. Guo, W. Zhang, Highly efficient interception and precipitation of uranium (VI) from aqueous solution by iron-electrocoagulation combined with cooperative chelation by organic ligands, Environ. Sci. Technol. 51 (24) (2017) 14368–14378.

[6] A. Kausar, M. Iqbal, A. Javed, K. Aftab, Z.-i.-H. Nazli, H.N. Bhatti, S. Nouren, Dyes adsorption using clay and modified clay: a review, J. Mol. Liq. 256 (2018) 395–407.

[7] M. Tuzen, A. Sarı, M.R. Afshar Mogaddam, S. Kaya, K.P. Katin, N. Altunay, Synthesis of carbon modified with polymer of diethylenetriamine and trimesoyl chloride for the dual removal of Hg (II) and methyl mercury ([CH3Hg]+) from wastewater: Theoretical and experimental analyses, Mater. Chem. Phys. 277 (2022) 125501, https://doi.org/10.1016/j.matchemphys.2021.125501.

[8] N. Tang, J. Liang, C. Niu, H. Wang, Y. Luo, W. Xing, S. Ye, C. Liang, H. Guo, J. Guo, Y. Zhang, G. Zeng, Amidoxime-based materials for uranium recovery and removal, J. Mater. Chem. A 8 (16) (2020) 7588–7625.

[9] S. Şimşek, U. Ulusoy, Adsorptive properties of sulfolignin–polyacrylamide graft copolymer for lead and uranium: effect of hydroxilamine–hydrochloride treatment, React. Funct. Polym. 73 (1) (2013) 73–82.

[10] Z. Zhang, Z. Dong, X. Wang, D. Ying, F. Niu, X. Cao, Y. Wang, R. Hua, Y. Liu, X. Wang, Ordered mesoporous polymer–carbon composites containing amidoxime groups for uranium removal from aqueous solutions, Chem. Eng. J. 341 (2018) 208–217.

[11] E. Padilla-Ortega, R. Leyva-Ramos, J. Mendoza-Barron, Role of electrostatic interactions in the adsorption of cadmium (II) from aqueous solution onto vermiculite, Appl. Clay Sci. 88-89 (2014) 10–17.

[12] S. Mao, T. Shen, T. Han, F. Ding, Q. Zhao, M. Gao, Adsorption and co-adsorption of chlorophenols and Cr (VI) by functional organo-vermiculite: Experiment and theoretical calculation, Sep. Purif. Technol. 277 (2021) 119638, https://doi.org/10.1016/j.seppur.2021.119638.

[13] W. Lv, T. Shen, F. Ding, S. Mao, Z. Ma, J. Xie, M. Gao, A novel NH_2-rich polymer/graphene oxide/organo-vermiculite adsorbent for the efficient removal of azo dyes, J. Mol. Liq. 341 (2021) 117308, https://doi.org/10.1016/j.molliq.2021.117308.

[14] S. Şİmşek, Adsorption properties of lignin containing bentonite-polyacrylamide composite for UO22+ ions, Desalin. Water Treat. 57 (50) (2016) 23790–23799.

[15] A.J. Domb, E.G. Cravalho, R. Langer, The synthesis of poly (hydroxamic acid) from poly (acrylamide), J. Polym. Sci., Part A: Polym. Chem. 26 (10) (1988) 2623–2630.

[16] I. Langmuir, The adsorption of gases on plane surfaces of glass, mica and platinum, J. Am. Chem. Soc. 40 (9) (1918) 1361–1403.

[17] H. Freundlich, W. Heller, The adsorption of cis-and trans-azobenzene, J. Am. Chem. Soc. 61 (8) (1939) 2228–2230.

[18] K.Y. Foo, B.H. Hameed, Insights into the modeling of adsorption isotherm systems, Chem. Eng. J. 156 (1) (2010) 2–10.

[19] J. Lin, L. Wang, Comparison between linear and non-linear forms of pseudo-first-order and pseudo-second-order adsorption kinetic models for the removal of methylene blue by activated carbon, Front. Environ. Sci. Eng. China 3 (3) (2009) 320–324.

[20] Y.S. Ho, G. McKay, Pseudo-second order model for sorption processes, Process Biochem. 34 (5) (1999) 451–465.

[21] Y.S. Ho, G. Mckay, Kinetic models for the sorption of dye from aqueous solution by wood, Process Saf. Environ. Prot. 76 (2) (1998) 183–191.

[22] O. Abollino, M. Aceto, M. Malandrino, C. Sarzanini, E. Mentasti, Adsorption of heavy metals on Na-montmorillonite. Effect of pH and organic substances, Water Res. 37 (7) (2003) 1619–1627.

[23] A.F. Belhaj, K.A. Elraies, S.M. Mahmood, N.N. Zulkifli, S. Akbari, O.S. Hussien, The effect of surfactant concentration, salinity, temperature, and pH on surfactant adsorption for chemical enhanced oil recovery: a review, J. Pet. Explor. Prod. Technol. 10 (1) (2020) 125–137.

[24] L.S. Čerović, S.K. Milonjić, M.B. Todorović, M.I. Trtanj, Y.S. Pogozhev, Y. Blagoveschenskii, E.A. Levashov, Point of zero charge of different carbides, Colloids Surf., A 297 (1-3) (2007) 1–6.

[25] G. Sposito, On points of zero charge, Environ. Sci. Technol. 32 (19) (1998) 2815–2819.

[26] D.L. Clark, S.D. Conradson, R.J. Donohoe, D.W. Keogh, D.E. Morris, P.D. Palmer, C.D. Tait, Chemical speciation of the uranyl ion under highly alkaline conditions. Synthesis, structures, and oxo ligand exchange dynamics, Inorg. Chem. 38 (7) (1999) 1456–1466.

[27] J.-H. Xue, H. Zhang, D.X. Ding, N. Hu, Y.-D. Wang, Y.-S. Wang, Linear β-cyclodextrin polymer functionalized multiwalled carbon nanotubes as nanoadsorbent for highly effective removal of U (VI) from aqueous solution based on inner-sphere surface complexation, Ind. Eng. Chem. Res. 58 (10) (2019) 4074–4083.

[28] L. Hao, H. Song, L. Zhang, X. Wan, Y. Tang, Y.i. Lv, SiO2/graphene composite for highly selective adsorption of Pb (II) ion, J. Colloid Interface Sci. 369 (1) (2012) 381–387.

[29] J. Zhang, D. Cai, G. Zhang, C. Cai, C. Zhang, G. Qiu, K. Zheng, Z. Wu, Adsorption of methylene blue from aqueous solution onto multiporous palygorskite modified by ion beam bombardment: Effect of contact time, temperature, pH and ionic strength, Appl. Clay Sci. 83-84 (2013) 137–143.

[30] R. Hsissou, R. Seghiri, Z. Benzekri, M. Hilali, M. Rafik, A. Elharfi, Polymer composite materials: A comprehensive review, Compos. Struct. 262 (2021) 113640, https://doi.org/10.1016/j.compstruct.2021.113640.

[31] R. Hsissou, A. Bekhta, O. Dagdag, A. El Bachiri, M. Rafik, A. Elharfi, Rheological properties of composite polymers and hybrid nanocomposites, Heliyon 6 (6) (2020) e04187, https://doi.org/10.1016/j.heliyon.2020.e04187.

[32] R. Hsissou, F. Benhiba, O. Dagdag, M. El Bouchti, K. Nouneh, M. Assouag, A. Elharfi, Development and potential performance of prepolymer in corrosion inhibition for carbon steel in 1.0 M HCl: outlooks from experimental and computational investigations, J. Colloid Interface Sci. 574 (2020) 43–60.

[33] Hsissou, Rachid, Fouad Benhiba, Said Abbout, Omar Dagdag, Said Benkhaya, Avni Berisha, Hamid Erramli, and Ahmed Elharfi. "Trifunctional epoxy polymer as corrosion inhibition material for carbon steel in 1.0 M HCl: MD simulations, DFT and complexation computations." *Inorganic Chemistry Communications* 115 (2020): 107858.

[34] I.B. Obot, S. Kaya, C. Kaya, B. Tüzün, Density Functional Theory (DFT) modeling and Monte Carlo simulation assessment of inhibition performance of some carbohydrazide Schiff bases for steel corrosion, Physica E 80 (2016) 82–90.

[35] N. Islam, S. Kaya (Eds.), Conceptual density functional theory and its application in the chemical domain, CRC Press, 2018.

[36] A. Dal Corso, Pseudopotentials periodic table: From H to Pu, Comput. Mater. Sci. 95 (2014) 337–350.

[37] P. Giannozzi, O. Andreussi, T. Brumme, O. Bunau, M. Buongiorno Nardelli, M. Calandra, R. Car, C. Cavazzoni, D. Ceresoli, M. Cococcioni, N. Colonna, I. Carnimeo, A. Dal Corso, S. de Gironcoli, P. Delugas, R.A. DiStasio, A. Ferretti, A. Floris, G. Fratesi, G. Fugallo, R. Gebauer, U. Gerstmann, F. Giustino, T. Gorni, J. Jia, M. Kawamura, H.-Y. Ko, A. Kokalj, E. Küçükbenli, M. Lazzeri, M. Marsili, N. Marzari, F. Mauri, N.L. Nguyen, H.-V. Nguyen, A. Otero-de-la-Roza, L. Paulatto, S. Poncé, D. Rocca, R. Sabatini, B. Santra, M. Schlipf, A.P. Seitsonen, A. Smogunov, I. Timrov, T. Thonhauser, P. Umari, N. Vast, X. Wu, S. Baroni, Advanced capabilities for materials modelling with Quantum ESPRESSO, J. Phys.: Condens. Matter 29 (46) (2017) 465901, https://doi.org/10.1088/1361-648X/aa8f79.

[38] Y. Kanai, X. Wang, A. Selloni, R. Car, Testing the TPSS meta-generalized-gradient-approximation exchange-correlation functional in calculations of transition states and reaction barriers, J. Chem. Phys. 125 (23) (2006) 234104, https://doi.org/10.1063/1.2403861.

[39] E.W.F. Smeets, J. Voss, G.-J. Kroes, Specific reaction parameter density functional based on the meta-generalized gradient approximation: application to H2+Cu (111) and H2+Ag (111), The Journal of Physical Chemistry A 123 (25) (2019) 5395–5406.

[40] S. Grimme, Semiempirical GGA-type density functional constructed with a long-range dispersion correction, J. Comput. Chem. 27 (15) (2006) 1787–1799.

[41] S. Kaya, C. Kaya, A new method for calculation of molecular hardness: a theoretical study, Comput. Theor. Chem. 1060 (2015) 66–70.

[42] S. Kaya, C. Kaya, A new equation for calculation of chemical hardness of groups and molecules, Mol. Phys. 113 (11) (2015) 1311–1319.

[43] R.G. Pearson, Hard and soft acids and bases, J. Am. Chem. Soc. 85 (22) (1963) 3533–3539.